JP Journal of Heat and Mass Transfer

http://www.pphmj.com
http://dx.doi.org/10.17654/0973576322058
Volume 30, 2022, Pages 89-104 **P-ISSN: 0973-5763**

EFFECT OF A MAGNETIC FIELD ON THE COUETTE FORCED CONVECTION OF A BUONGIORNO'S NANOFLUID OVER AN EMBEDDED CAVITY

Abderrahim Mokhefi and Eugenia Rossi di Schio

Mechanics, Modeling and Experimentation Laboratory L2ME
Faculty of Technology
Bechar University
B.P. 417, Bechar 08000, Algeria
e-mail: abderrahim.mokhefi@univ-bechar.dz

Department of Industrial Engineering DIN
Alma Mater Studiorum - University of Bologna
Viale Risorgimento 2, I-40136 Bologna, Italy
e-mail: eugenia.rossidischio@unibo.it

Abstract

The paper investigates the effect of a magnetic field on the forced convection of a nanofluid in a channel with an embedded cavity. The nanofluid is described by the Buongiorno's model, and a fixed temperature boundary condition is prescribed. The governing

Received: October 6, 2022; Accepted: November 7, 2022

Keywords and phrases: nanofluid Buongiorno's model, embedded cavity, forced convection, magnetic field.

How to cite this article: Abderrahim Mokhefi and Eugenia Rossi di Schio, Effect of a magnetic field on the Couette forced convection of a Buongiorno's nanofluid over an embedded cavity, JP Journal of Heat and Mass Transfer 30 (2022), 89-104.
http://dx.doi.org/10.17654/0973576322058

Published Online: December 15, 2022

equations are written in a dimensionless form and solved numerically by employing COMSOL Multiphysics. The obtained velocity, temperature and concentration fields are presented as function of the governing parameters, and the Nusselt number on the upper boundary is evaluated as well. Particular attention is paid to the effect of the inclination angle of the magnetic field, showing that variations up to 40% may affect the Nusselt number.

1. Introduction

Nowadays, nanofluids are employed, and even expected to increase their role, in heat transfer because they exhibit enhanced thermal conductivity and enhanced convective heat transfer coefficient compared to the base fluid [1]. According to the model introduced by Buongiorno [2], the main features that characterize the nanofluid behavior are thermophoresis and Brownian diffusion and recent studies investigate and digest the modelling of laminar nanofluid flow, both with reference to a clear nanofluid [3] or to a nanofluid saturating a porous medium [4-6].

Recently, many authors investigated the effect of a magnetic field on the mixed convection of a nanofluid, both for uniform [7] and non-uniform magnetic field [8], or with reference to a cavity [9]. The Marangoni effect has been investigated by Rehman et al. [10], while in [11] slip boundary conditions and an oscillating boundary condition are taken into account. Concerning slip boundary condition, the Couette flow of a nanofluid in a channel with an embedded cavity has been investigated in [12], while in [13] for the same geometry the vortex formation of a clear fluid is discussed.

In the present paper, we investigate the forced convection of a nanofluid in a channel with an embedded cavity. The thermal boundary conditions are given by two different temperature values prescribed on the lower boundary and on the upper boundary; a uniform inlet concentration of nanoparticles is assumed, and the inlet velocity is prescribed as a linear function of the vertical coordinate. The effect of a magnetic field is investigated by introducing the dimensionless Hartmann number, and the Nusselt number is

evaluated as a function of the Reynolds number, for different Hartmann number as well as different inclination angle of the magnetic field at fixed Prandtl number, Lewis number and thermophoresis and Brownian diffusion parameters. The consideration of the magnetic field in the present investigation is, on the one hand, part of an improvement step of the modeling in the case where an electrically conductive nanofluid is in a medium subject to leakage of magnetic field lines generated by electrical equipment. On the other hand, it is part of an in-depth analysis aiming at extracting the impact of the Lorentz force on the heat exchange rate within a channel with an embedded cavity.

2. Setting of the Model

Let us consider a nanofluid, described by the Buongiorno's model [2], that steadily flows in forced convection regime in a duct with an embedded cavity as shown in Figure 1. Following the same procedure described in [12], we solve the dimensionless equations for mass, momentum, energy and nanoparticles balances. In addition to the case studied in [12], in the present study the flow of the nanofluid is subject to a force due to a constant intensity of a magnetic field B at different angles γ. Indeed, in the source term of the momentum equation, the magnetic force is introduced based on the theory of magnetohydrodynamics [14].

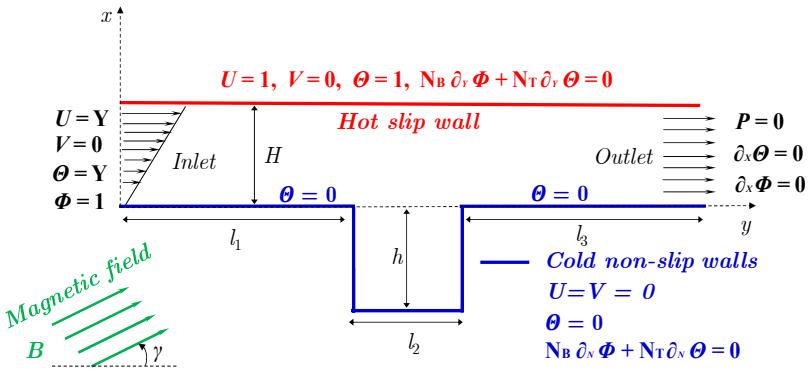

Figure 1. Sketch of the domain with boundary conditions and magnetic field.

In a Cartesian reference frame (OXY), the dimensionless mass, momentum, energy and nanoparticle concentration balances are given by

$$\frac{\partial U}{\partial X} + \frac{\partial V}{\partial Y} = 0, \tag{1}$$

$$U\frac{\partial U}{\partial X} + V\frac{\partial U}{\partial Y} = -\frac{\partial P}{\partial X} + \frac{1}{Re}\left(\frac{\partial^2 U}{\partial X^2} + \frac{\partial^2 U}{\partial Y^2}\right) + \frac{Ha^2}{Re}(V\cos\gamma\sin\gamma - U\sin^2\gamma), \tag{2}$$

$$U\frac{\partial V}{\partial X} + V\frac{\partial V}{\partial Y} = -\frac{\partial P}{\partial X} + \frac{1}{Re}\left(\frac{\partial^2 V}{\partial X^2} + \frac{\partial^2 V}{\partial Y^2}\right) + \frac{Ha^2}{Re}(U\cos\gamma\sin\gamma - V\cos^2\gamma), \tag{3}$$

$$U\frac{\partial \Theta}{\partial X} + V\frac{\partial \Theta}{\partial Y} = \frac{1}{RePr}\left(\frac{\partial^2 \Theta}{\partial X^2} + \frac{\partial^2 \Theta}{\partial Y^2}\right) + \frac{1}{Re.Pr}\left[N_B\left(\frac{\partial \Theta}{\partial X}\frac{\partial \Phi}{\partial X} + \frac{\partial \Theta}{\partial Y}\frac{\partial \Phi}{\partial Y}\right) + N_T\left(\left(\frac{\partial \Theta}{\partial X}\right)^2 + \left(\frac{\partial \Theta}{\partial Y}\right)^2\right)\right], \tag{4}$$

$$U\frac{\partial \Phi}{\partial X} + V\frac{\partial \Phi}{\partial Y} = \frac{1}{Re.Pr.Le}\left[\left(\frac{\partial^2 \Phi}{\partial X^2} + \frac{\partial^2 \Phi}{\partial Y^2}\right) + \frac{N_T}{N_B}\left(\frac{\partial^2 \Theta}{\partial X^2} + \frac{\partial^2 \Theta}{\partial Y^2}\right)\right]. \tag{5}$$

In equations (1)-(5), (U, V), P, Θ and Φ are respectively the dimensionless: velocity coordinates, pressure, temperature and concentration. Re, Pr, Le, Ha, N_B and N_T denote: Reynolds number, Prandtl number, Lewis number, Hartmann number, Brownian motion parameter and thermophoresis parameter (respectively). In particular, the Hartmann number accounts on the variation of the intensity in terms of magnetic field.

The dimensionless variables and parameters are defined as follows:

$$(X,\,Y)=\frac{(x,\,y)}{H},\,(U,\,V)=\frac{(u,\,v)}{u_0},\,p=\frac{\overline{p}}{\rho u_0^2},\,\Theta=\frac{T-T_c}{T_h-T_c},\,\Phi=\frac{\varphi}{\varphi_0}. \quad (6)$$

As shown in Figure 1, the dimensionless boundary conditions are:

$$\textit{Inlet}:\ U=Y,\,V=0,\,\Theta=Y,\,\Phi=1, \quad (7)$$

$$\textit{Outlet}:\ P=0,\,\frac{\partial\Theta}{\partial X}=\frac{\partial\Phi}{\partial X}=0, \quad (8)$$

$$\textit{Hot wall}:\ U=1,\,V=0,\,\Theta=1,\,N_B\frac{\partial\Phi}{\partial Y}+N_T\frac{\partial\Theta}{\partial Y}=0, \quad (9)$$

$$\textit{Horizontal cold walls}:\ U=V=\Theta=0,\,N_B\frac{\partial\Phi}{\partial Y}+N_T\frac{\partial\Theta}{\partial Y}=0, \quad (10)$$

$$\textit{Vertical cold walls}:\ U=V=\Theta=0,\,N_B\frac{\partial\Phi}{\partial X}+N_T\frac{\partial\Theta}{\partial X}=0. \quad (11)$$

The dimensionless stream function is determined by solving the following equation:

$$\frac{\partial^2\Psi}{\partial X^2}+\frac{\partial^2\Psi}{\partial Y^2}=\frac{\partial U}{\partial Y}-\frac{\partial V}{\partial X}. \quad (12)$$

Finally, in order to calculate the heat transfer rate, an average Nusselt number is defined as

$$Nu_{avg}=\frac{H}{L}\int_0^{L/H}\frac{\partial\Theta}{\partial Y}\,dX. \quad (13)$$

3. Numerical Procedure and Validation

The governing dimensionless equations (1)-(5) with the boundary conditions (7)-(11) are discretized using the Galerkin finite element method integrated in COMSOL Multiphysics 6.0 software. After having chosen a

uniform quadratic mesh shown in Figure 2, an independence test of the various numerical results from this mesh has been performed. Thus, it has been opted for a grid containing 77826 quadratic domain elements beyond which the numerical results remain unchanged. The solution converges when the relative error between the new and old values of velocity components, pressure, temperature and concentration become less than 10^{-6}.

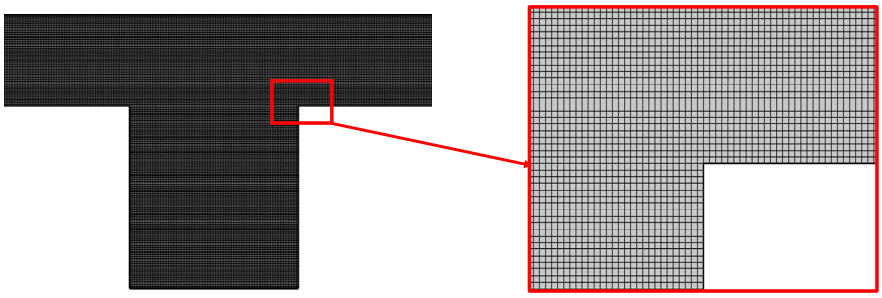

Figure 2. Mesh of the computation domain.

Table 1. Comparison of the average Nusselt number of the present study with the reference for $Ha = 25$ and an average volume fraction of 0.05

Inclination angle [°]	0	30	60	90
Ref. [15]	2.528	4.157	4.766	4.942
Present results	2.526	4.153	4.765	4.933
% difference	0.07	0.09	0.02	0.18

To ensure the consistency of the present numerical results, a comparison with data available in the literature and based on a similar topic is done. In [15], Hussain and Ahmed studied the influence of the magnetic field and its inclination angle in the case of forced convection. By applying the same conditions, we compared the values of the average Nusselt number for various inclination angles. Table 1 shows the values of the Nusselt number from the present code and those extracted from the graphs of ref. [15]. The comparison shows that there is a very good agreement with a deviation percentage that did not exceed 0.18%.

4. Results

In this section, the results of the numerical simulation of the forced flow of a nanofluid in a channel with an embedded cavity are presented. The influences of the intensity of a uniform magnetic flux density represented by the Hartmann number $(Ha = 0 \text{ to } 100)$ as well as of the inclination angle of the magnetic field with respect to the horizontal line $(\gamma = 0^\circ \text{ to } 90^\circ)$ on the hydrodynamic and thermal states and on the distribution of nanoparticles are investigated. The Reynolds, Prandtl and Lewis numbers as well as the parameters of Brownian motion and thermophoresis are respectively fixed at: $Re = 100$, $Pr = 6.2$, $Le = 10$, $N_B = 0.1$ and $N_T = 0.1$ [12].

4.1. Effect of Hartmann number

Figure 3 illustrates the streamlines patterns as well as the dimensionless temperature and concentration contours in the extended part of the channel for different values of the Hartmann number. The angle of inclination of the magnetic field is fixed at 45°.

In absence of the magnetic field, the streamlines are subject to the fluid flow rate entering the channel and a wide recirculation zone due to the flow reattachment occurs in the embedded cavity. By introducing a uniform magnetic field with increasing flux densities, the structure of the flow radically changes. Indeed, a formation of a recirculation zone in the vicinity of the corner opposite to the flow occurs. With the increase of the Hartmann number this recirculation zone widens diagonally by virtue of the inclination of the applied magnetic field and increases in terms of number and intensity of flow (the minimum stream function increases from 0.47 to 0.5 except in the case of $Ha = 100$ this function decreases to 0.49). Regarding the thermal and mass structures, the isotherms and the iso-concentrations are almost similar to the streamlines. On the other hand, the hot thermal profile tended to move downwards or towards the embedded cavity with the increase of the Hartmann number.

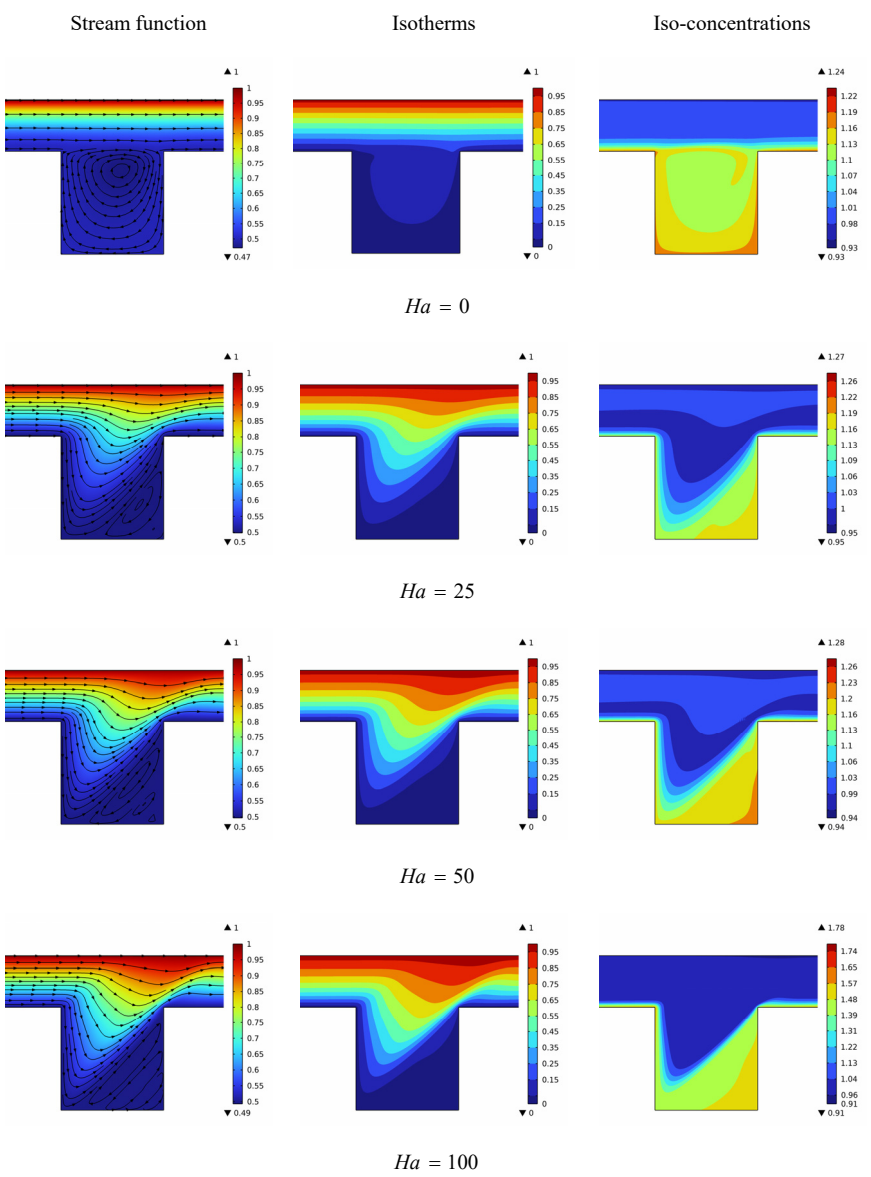

Figure 3. Stream function, isotherms and iso-concentration for different values of Hartmann number at $Re = 100$, $Pr = 6.2$, $Le = 10$, $N_B = N_T = 0.1$ and $\gamma = 45^{\circ}$.

The distribution of nanoparticles is also influenced by the introduction of the magnetic field with increasing intensity. Following the direction of the Lorenz force perpendicular to the magnetic field, the nanoparticles concentration increases in the vicinity of the cavity corner opposite flow direction. Moreover, the rate of accumulation and the nanoparticles migration to this area increases as the Hartmann number increases.

Figure 4 shows the dimensionless distribution of the nanoparticle concentration, temperature as well as the vertical coordinate of the nanofluid velocity along the vertical median line through the embedded cavity for different values of the Hartmann number. For increasing values of Ha, the nanoparticles concentration increases in the lower part of the cavity $(Y = -2)$, while it remains almost the same next to the upper walls $(Y = 1)$. On the other hand, the distribution of nanoparticles becomes more homogeneous in the majority of this direction as the Hartmann number increases. The temperature distribution along the vertical median line increases for increasing Hartmann number. Regardless of the value of the Hartmann number, along the measurement line, the temperature increases from the lower wall of the cavity towards the upper moving wall of the channel $(Y = -2 \text{ to } 1)$. The thermal gradient is low in the part of the vertical line crossing the embedded cavity $(Y = -2 \text{ to } 0)$, while it is important in the part crossing the channel $(Y = 0 \text{ to } 1)$. In the case of increasing intensity of the magnetic field, the temperature increases rapidly in the whole vertical line including the cavity. Indeed, the change in this pattern is mainly due to the increase in the vertical coordinate of the velocity, especially in the upper part, which was almost absent in the case of $Ha = 0$, see Figure 4(c).

Figure 5 presents the average Nusselt number as a function of the Reynolds number for different values of Hartmann number. For $Ha = 0$, the Nusselt number is an increasing function of *Re*: indeed, a rise of the heat exchange rate occurs with the increase of the inlet velocity.

With the introduction of the magnetic field, for all Reynolds numbers, the average Nusselt number decreases significantly with the increase of *Ha*, especially at $Ha = 100$. On the other hand, in presence of the magnetic field, the average Nusselt number decreases as a function of *Re* number until a critical value beyond which it starts to increase. This is due to the predominance of inertia over magnetism more than specified Reynolds numbers.

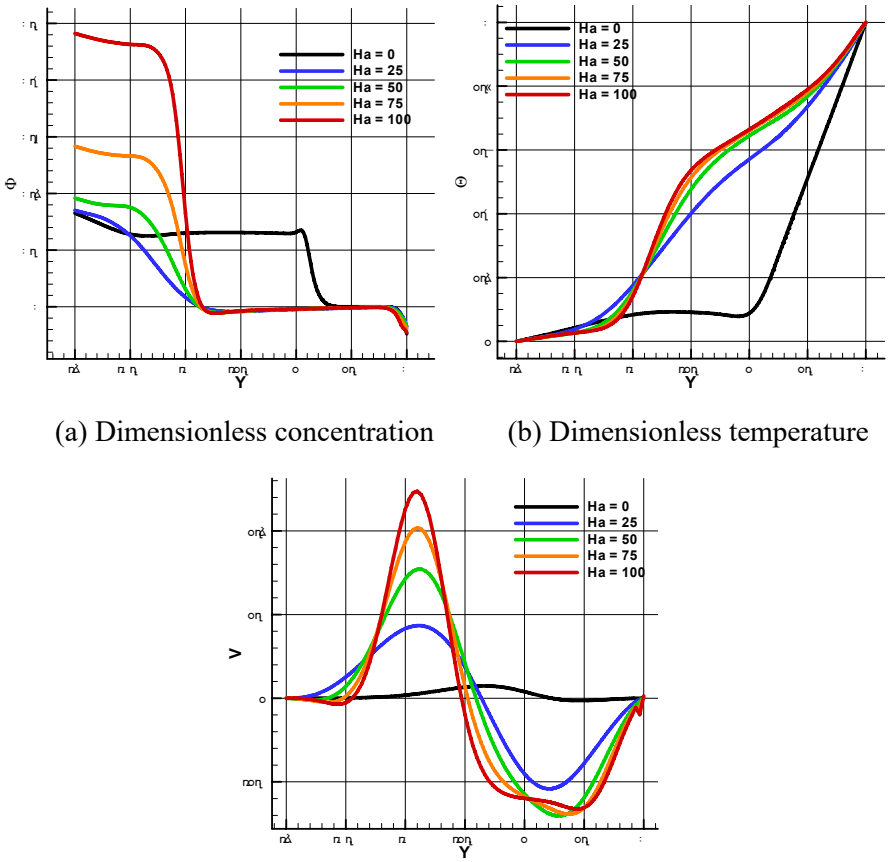

(a) Dimensionless concentration (b) Dimensionless temperature

(c) Dimensionless velocity

Figure 4. Concentration, temperature and velocity along the vertical direction for different values of *Ha* at $Re = 100$, $Pr = 6.2$, $Le = 10$, $N_B = N_T = 0.1$ and $\gamma = 45^{\circ}$.

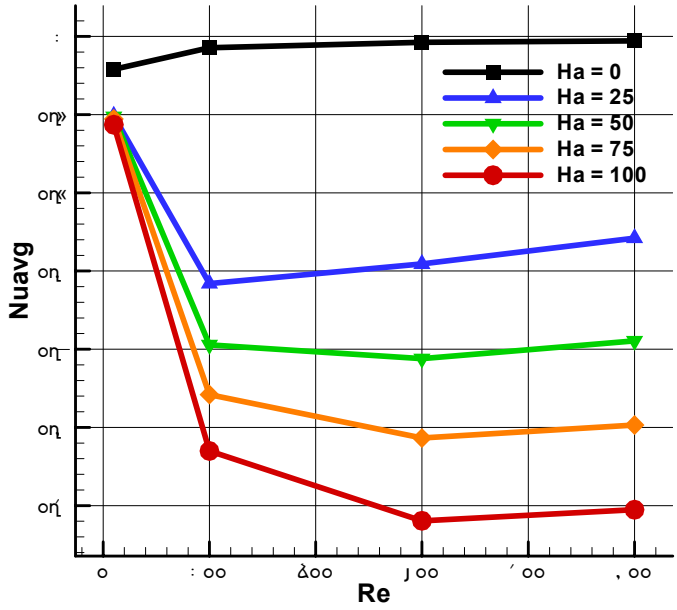

Figure 5. Average Nusselt number as function of Reynolds number for different values of Hartmann number at $Pr = 6.2$, $Le = 10$, $N_B = N_T = 0.1$ and $\gamma = 45^{\circ}$.

4.2. Effect of inclination angle of the magnetic field

Figure 6 shows the streamlines and the distribution of temperature and nanoparticles concentration in the region of the channel containing the embedded cavity, for different inclination angles of the magnetic field. The Hartmann number in this case is set at $Ha = 50$. For a horizontal magnetic field $(\gamma = 0^{\circ})$, four vertically superposed recirculation zones are developed in the embedded cavity. By inclining the magnetic field with different angles, the recirculation zones tilt proportionally with the magnetic force.

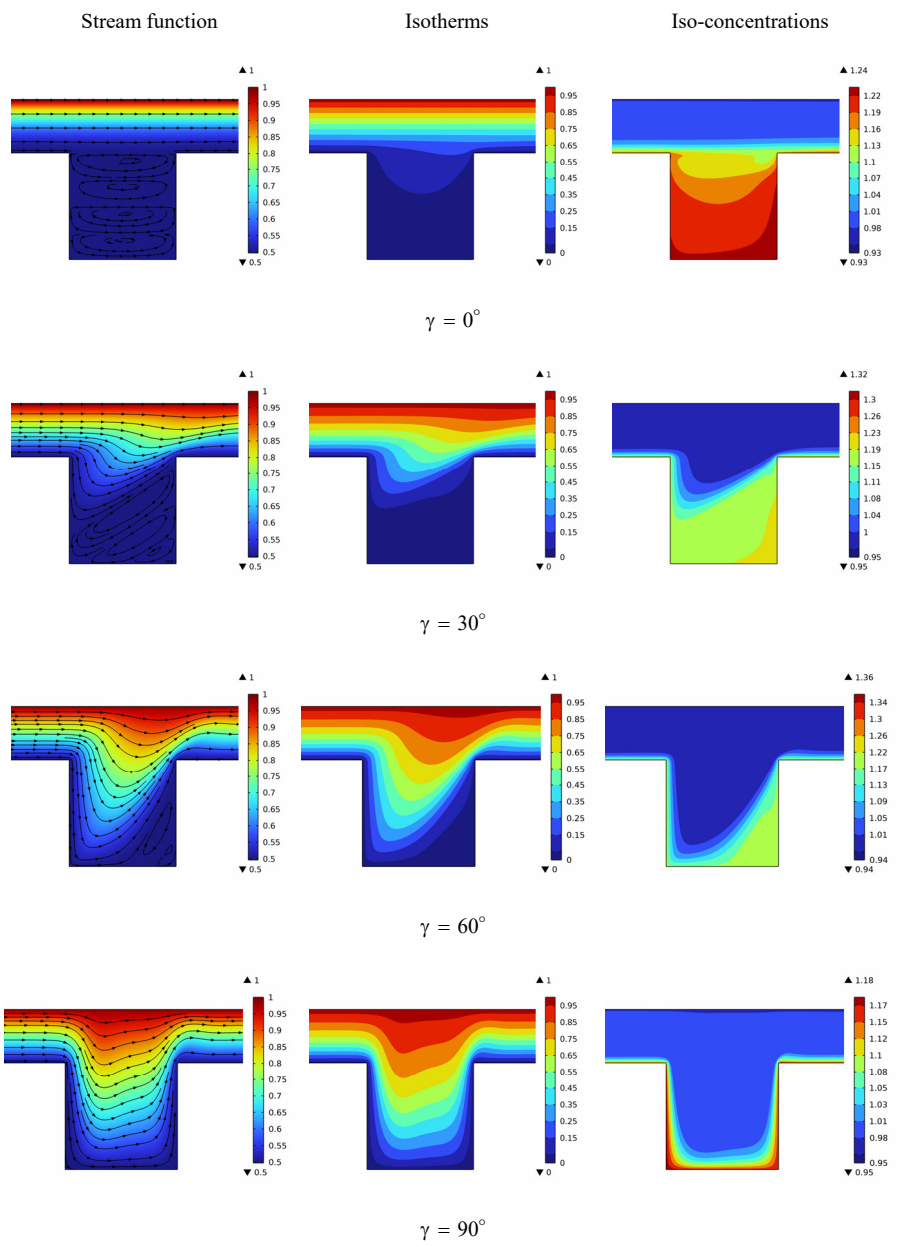

Figure 6. Stream function, isotherms and iso-concentration for different inclination angle of magnetic field at $Re = 100$, $Pr = 6.2$, $Le = 10$, $N_B = N_T = 0.1$ and $Ha = 50$.

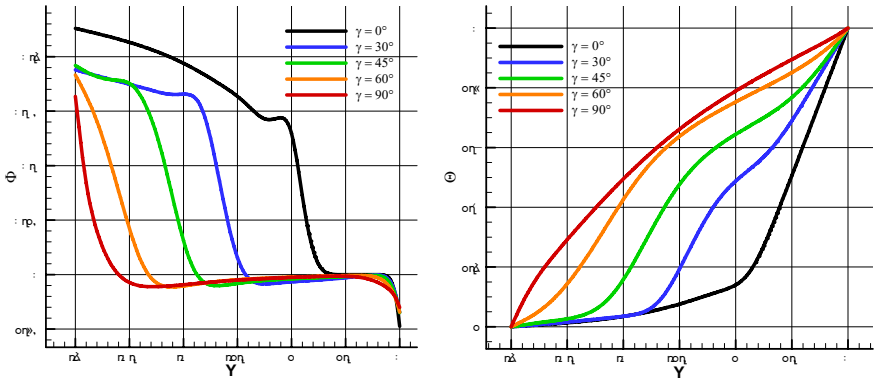

(a) Dimensionless concentration (b) Dimensionless temperature

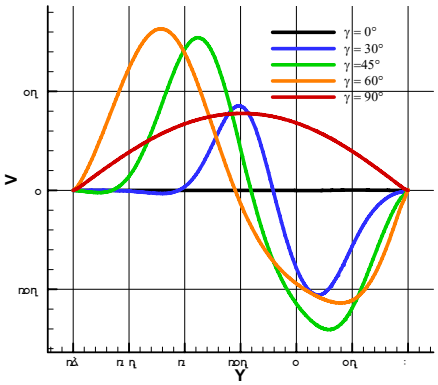

(c) Dimensionless velocity

Figure 7. Concentration, temperature and velocity along the vertical direction for different values of inclination angle of magnetic field at $Re = 100$, $Pr = 6.2$, $Le = 10$, $N_B = N_T = 0.1$ and $Ha = 50$.

Moreover, the vortexes arrange themselves according to the direction of the magnetic force and decrease in number and size until they disappear completely in the case of $\gamma = 90^{\circ}$. In this last case, the flow is complete without vortexes in the whole cavity. On the other hand, the temperature contours follow the form of the streamlines. Indeed, the length of the thermal boundary layer in this area increases by tilting the magnetic field to the angle $\gamma = 90^{\circ}$. Also, the concentration distribution of nanoparticles follows the

hydrodynamic and thermal structure. In addition to thermophoretic migration, the distribution of nanoparticles strongly follows the direction of the magnetic force. On the other hand, in the case of an angle of $\gamma = 90^{\circ}$ the migration of nanoparticles occurs by purely thermophoretic diffusion.

Figure 7 displays the nanoparticle concentration and temperature distribution, as well as the vertical coordinate of the velocity along the vertical median line, for different inclination angles of the magnetic field. A decrease in the concentration at the bottom of the cavity occurs for increasing values of the inclination angle of the magnetic field, from 0° to 90°. A particular homogenization in the distribution of nanoparticles along this direction arises when $\gamma = 90^{\circ}$. On the other hand, the temperature rises with the increase of the inclination angle.

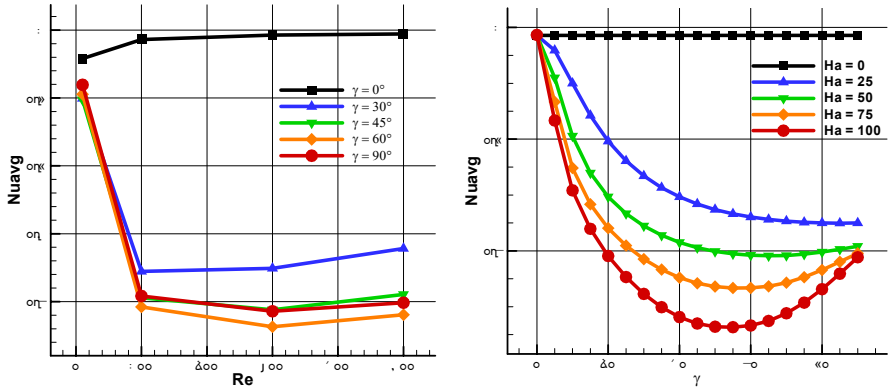

(a) (b)

Figure 8. Average Nusselt number at $Pr = 6.2$, $Le = 10$, $N_B = N_T = 0.1$: (a) as function of Reynolds number for different inclination angle of magnetic field at $Ha = 50$; (b) as function of the inclination angle for different Hartmann numbers at $Re = 100$.

Finally, Figure 8 shows the variation of the average Nusselt number as a function of Reynolds number for different inclination angles (frame (a)) and as a function of the inclination angle for different values of *Ha* (frame (b)). The inclination angle negatively affects the Nusselt number especially in the case of $\gamma = 60^{\circ}$. Frame (b) shows that the inclination angle does not always

negatively affect the heat transfer. Indeed, in the presence of a magnetic field, especially at a high intensity, the increase of the inclination angle from 0° to a critical value leads to a decrease of the Nusselt number, then beyond this angle the Nusselt number increases.

5. Conclusions

In the present paper, the effect of a magnetic field on the forced convection of a nanofluid in a channel with an embedded cavity is presented. Reference is made to Buongiorno's model, and the dimensionless equations are solved employing the software package COMSOL Multiphysics. Particular attention is paid to the role of the inclination of the magnetic field, showing that variations up to 40% may affect the Nusselt number. Moreover, while in case of horizontal magnetic field the average Nusselt number is an increasing monotonic function of the Reynolds number, this does not happen when different inclinations are investigated.

References

[1] S. Kakaç and P. Anchasa, Review of convective heat transfer enhancement with nanofluids, International Journal of Heat and Mass Transfer 52 (2009), 3187-3196. Doi: 10.1016/j.ijheatmasstransfer.2009.02.006

[2] J. Buongiorno, Convective transport in nanofluids, Journal of Heat Transfer 128 (2006), 240-250. https://doi.org/10.1115/1.2150834

[3] E. R. D. Schio, M. Celli and A. Barletta, Effects of Brownian diffusion and thermophoresis on the laminar forced convection of a nanofluid in a channel, Journal of Heat Transfer 136 (2014), 022401. https://doi.org/10.1115/1.4025376

[4] A. Barletta, E. R. Di Schio and M. Celli, Convection and Instability Phenomena in Nanofluid-saturated Porous Media, Heat Transfer Enhancement with Nanofluids, V. Bianco, O. Manca, S. Nardini and K. Vafai, eds., CRC Press, Boca Raton, USA, 2015, pp. 341-364.

[5] E. R. Di Schio, Analysis of the forced convection in a porous channel saturated by a nanofluid: effects of Brownian diffusion and thermophoresis, ASME International Mechanical Engineering Congress and Exposition, Proceedings (IMECE), 2014. Doi: 10.1115/IMECE2014-39634

[6] E. R. Di Schio, The thermal entrance region in a porous medium saturated by a nanofluid: Analysis of the Brinkman's model, Journal of Physics: Conference Series 547 (2014), 012022.

[7] M. Sheikholeslami and M. M. Bhatti, Forced convection of nanofluid in presence of constant magnetic field considering shape effects of nanoparticles, International Journal of Heat and Mass Transfer 111 (2017), 1039-1049.

[8] M. Sheikholeslami, M. M. Rashidi and D. D. Ganji, Effect of non-uniform magnetic field on forced convection heat transfer of Fe_3O_4-water nanofluid, Computer Methods in Applied Mechanics and Engineering 294 (2015), 299-312.

[9] M. Sheikholeslami, Influence of magnetic field on Al_2O_3-H_2O nanofluid forced convection heat transfer in a porous lid driven cavity with hot sphere obstacle by means of LBM, Journal of Molecular Liquids 263 (2018), 472-488.

[10] A. Rehman, Z. Salleh and T. Gul, The impact of Marangoni convection, magnetic field and viscous dissipation on the thin film unsteady flow of go-eg/go-w nanofluids over an extending sheet, JP Journal of Heat and Mass Transfer 18(2) (2019), 477-496.

[11] Z. Nikkhah, A. Karimipour, M. R. Safaei, P. Forghani-Tehrani, M. Goodarzi, M. Dahari and S. Wongwises, Forced convective heat transfer of water/functionalized multi-walled carbon nanotube nanofluids in a microchannel with oscillating heat flux and slip boundary condition, International Communications in Heat and Mass Transfer 68 (2015), 69-77.

[12] E. Rossi di Schio, A. N. Impiombato, A. Mokhefi and C. Biserni, Theoretical and numerical study on Buongiorno's model with a Couette flow of a nanofluid in a channel with an embedded cavity, Applied Sciences 12 (2022), 7751. https://doi.org/10.3390/app12157751

[13] C. Biserni, A. N. Impiombato, A. Jahanbin, E. R. Di Schio and G. Semprini, Formation and topology of vortices in Couette flow over open cavities, E3S Web of Conferences 197 (2020), pp. 10005. https://doi.org/10.1051/e3sconf/202019710005

[14] J. P. Freidberg, Ideal Magnetohydrodynamics, Plenum Publishing Corp., New York, NY, 1987.

[15] S. Hussain and S. E. Ahmed, Unsteady MHD forced convection over a backward facing step including a rotating cylinder utilizing Fe_3O_4-water ferrofluid, Journal of Magnetism and Magnetic Materials 484 (2019), 356-366. https://doi.org/10.1016/j.jmmm.2019.04.040